

# Ecological and evolutionary implications of starvation and body size

1 **Justin D. Yeakel \* †‡, Christopher P. Kempes †, and Sidney Redner †§**

4 \*School of Natural Science, University of California Merced, Merced, CA, †The Santa Fe Institute, Santa Fe, NM, §Department of Physics, Boston University, Boston  
5 MA, and ‡To whom correspondence should be addressed: jdyeakel@gmail.com

6 Submitted to Proceedings of the National Academy of Sciences of the United States of America

7 **This is the abstract.** No it isn't. It's merely a placeholder.

8 foraging | starvation | reproduction

## 9 Introduction

10 The behavioral ecology of most, if not all, organisms is influ-  
11 enced by the energetic state of individuals, which directly influ-  
12 ences how organisms invest reserves in uncertain environments.  
13 Such behaviors are generally manifested as trade-offs between  
14 investing in somatic maintenance and growth or allocating en-  
15 ergy towards reproduction [1, 2, 3]. The timing of these be-  
16 haviors responds to selective pressure, as the choice of the in-  
17 vestment impacts future fitness! [4]. The influence of resource  
18 limitation on an organism's ability to maintain its nutritional  
19 stores may lead to repeated delays or shifts in reproduction over  
20 the course of an organism's life.

21 The life history of most species is typically comprised of (a)  
22 somatic growth and maintenance and (b) reproduction. The  
23 balance between these two activities is often conditioned on  
24 resource availability [5]. For example, reindeer invest less in  
25 calves born after harsh winters (when the mother's energetic  
26 state is depleted) than in calves born after moderate winters [6].  
27 Many bird species invest differently in broods during periods  
28 of resource scarcity compared to normal periods [7, 8], some-  
29 times delaying or even foregoing reproduction for a breeding  
30 season [1, 9, 10]. Even freshwater and marine zooplankton have  
31 been observed to avoid reproduction under nutritional stress  
32 [11], and those that do reproduce have lower survival rates [2].  
33 Organisms may also separate maintenance and growth from re-  
34 production over space and time: many salmonids, birds, and  
35 some mammals return to migratory breeding grounds to repro-  
36 duce after one or multiple seasons in resource-rich environments  
37 where they accumulate nutritional reserves [12, 13, 14].

38 Physiological mechanisms also play an important role in reg-  
39 ulating reproductive expenditures during periods of resource  
40 limitation. Diverse mammals (47 species in 10 families) ex-  
41 hibit delayed implantation, whereby females postpone fetal  
42 development (blastocyst implantation) until times where nu-  
43 tritional reserves can be accumulated [15, 16]. Many other  
44 many species (including humans) suffer irregular menstrual cy-  
45 cling and higher abortion rates during periods of nutritional  
46 stress [17, 18]. In the extreme case of unicellular organisms,  
47 nutrition is unavoidably linked to reproduction because the nu-  
48 tritional state of the cell regulates all aspects of the cell cycle  
49 [19]. The existence of so many independently evolved mechan-  
50 isms across such a diverse suite of organisms highlights the im-  
51 portance and universality of the fundamental tradeoff between  
52 somatic and reproductive investment. However the dynamic  
53 implications of these constraints are unknown.

54 Though straightforward conceptually, incorporating the en-  
55 ergetic dynamics of individuals [20] into a population-level  
56 framework [20, 21] presents numerous mathematical obsta-  
57 cles [22]. An alternative approach involves modeling the  
58 macroscale relations that guide somatic versus reproductive  
59 investment in a consumer-resource system. For example,  
60 macroscale Lotka-Volterra models assume that the growth rate

61 of the consumer population depends on resource density, thus  
62 *implicitly* incorporating the requirement of resource availability  
63 for reproduction [23].

64 In this work, we adopt an alternative approach in which re-  
65 source limitation and the subsequent effect of starvation is ac-  
66 counted for *explicitly*. Namely, only individuals with sufficient  
67 energetic reserves can reproduce. Such a constraint leads to  
68 reproductive time lags due to some members of the population  
69 starving and then recovering. Additionally, we incorporate the  
70 idea that reproduction is strongly constrained allometrically [3],  
71 and is not generally linearly related to resource density. As we  
72 shall show, these constraints influence the ensuing population  
73 dynamics in dramatic ways.

## 74 Nutritional-state-structured model (NSM)

75 We begin by defining a minimal Nutritional-State-  
76 structured population Model (NSM), where the consumer pop-  
77 ulation is divided into two energetic states: (a) an energetically  
78 replete (full) state  $F$ , where the consumer reproduces at a con-  
79 stant rate  $\lambda$ , and (b) an energetically deficient (hungry) state  
80  $H$ , where the consumer does not reproduce but dies at rate  $\mu$ .  
81 The underlying resource  $R$  evolves by logistic growth with an  
82 intrinsic growth rate  $\alpha$  and a carrying capacity equal to one.  
83 Consumers transition from the full state  $F$  to the hungry state  
84  $H$  by starvation at rate  $\sigma$  and also in proportion to the absence  
85 of resources  $(1 - R)$ . Conversely, consumers recover from state  
86  $H$  to state  $F$  at rate  $\rho$  and in proportion to  $R$ . Resources are  
87 also eaten by the consumers—at rate  $\rho$  by hungry consumers  
88 and at rate  $\beta < \rho$  by full consumers. This inequality accounts  
89 for hungry consumers requiring more resources to rebuild body  
90 weight.

90 In the mean-field approximation, in which the consumers  
91 and resources are perfectly mixed, their densities evolve accord-  
92 ing to the rate equations

$$\begin{aligned}\dot{F} &= \lambda F + \rho RH - \sigma(1 - R)F, \\ \dot{H} &= \sigma(1 - R)F - \rho RH - \mu H, \\ \dot{R} &= \alpha R(1 - R) - R(\rho H + \beta F).\end{aligned}\quad [1]$$

93 Notice that the total consumer density  $F + H$  evolves accord-  
94 ing to  $\dot{F} + \dot{H} = \lambda F - \mu H$ . This resembles the equation of  
95 motion for the predator density in the classic Lotka-Volterra  
96 model, except that the resource density does not appear in the

## Reserved for Publication Footnotes

99 growth term. As discussed above, the attributes of reproduction and mortality have been explicitly apportioned to the full 100 and hungry consumers, respectively, so that the growth in the total density is decoupled from the resource density.

103 Equation [1] has three fixed points: two trivial fixed points at  $(F^*, H^*, R^*) = (0, 0, 0)$  and  $(0, 0, 1)$ , and one non-trivial, 104 internal fixed point at

$$\begin{aligned} F^* &= \frac{\alpha\lambda\mu(\mu + \rho)}{(\lambda\rho + \mu\sigma)(\lambda\rho + \mu\beta)}, \\ H^* &= \frac{\alpha\lambda^2(\mu + \rho)}{(\lambda\rho + \mu\sigma)(\lambda\rho + \mu\beta)}, \\ R^* &= \frac{\mu(\sigma - \lambda)}{\lambda\rho + \mu\sigma}. \end{aligned}$$

106 If this internal fixed point, which is unique, is stable, it will 107 be the global attractor for all population trajectories for any 108 initial condition where the resource and consumer densities are 109 both non zero. The stability of this fixed point is determined by 110 the Jacobian Matrix  $\mathbf{J}$ , where each matrix element  $J_{ij}$  equals 111  $\partial\dot{X}_i/\partial X_j$  when evaluated at the internal fixed point, and  $\mathbf{X}$  is 112 the vector  $(F, H, R)$ . If the parameters in Eq. [1] are such that 113 the real part of the largest eigenvalue of  $\mathbf{J}$  is negative, then the 114 system is stable with respect to small perturbations from the 115 fixed point.

116 From Eq. [2], an obvious constraint on the NSM is that 117 the reproduction rate  $\lambda$  must be less than the starvation rate 118  $\sigma$ , so that  $R^*$  is positive. Moreover, when the resource density 119  $R = 0$ , the rate equation for  $F$  gives exponential growth for 120  $\lambda > \sigma$ . The condition  $\sigma = \lambda$  represents a transcritical (TC) bi- 121 furcation that demarcates the physical and unphysical regimes. 122 The biological implication of the constraint  $\lambda < \sigma$  is simple— 123 the rate at which a macroscopic organism loses mass due to 124 lack of resources is generally much faster than the rate of repro- 125 duction. As we will discuss below, this inequality is a natural 126 consequence of allometric constraints [3] for organisms within 127 empirically observed body size ranges (Fig. 2).

128 In the physical regime of  $\lambda < \sigma$ , the fixed point [2] may 129 either be a stable node or a limit cycle (Fig. 3). In continuous- 130 time systems, a limit cycle arises when a pair of complex con- 131 jugate eigenvalues crosses the imaginary axis to attain positive 132 real parts [28]. This Hopf bifurcation is defined by  $\text{Det}(\mathbf{S}) = 0$ , 133 where  $\mathbf{S}$  is the Sylvester matrix, which is composed of the co- 134 efficients of the characteristic polynomial of the Jacobian ma- 135 trix [29]. As the system parameters are tuned to be within the 136 stable regime but close to the Hopf bifurcation, the amplitude 137 of the transient but decaying cycles become large. Given that 138 ecological systems are constantly being perturbed [30], the on- 139 set of transient cycles, even though they decay with time, can 140 increase the extinction risk [31, 32, 33]. Thus the distance of 141 a system from the Hopf bifurcation provides a measure of its 142 persistence.

143 When the starvation rate  $\sigma \gg \lambda$ , a substantial fraction 144 of the consumers are driven to the hungry non-reproductive 145 state. Because reproduction is inhibited, there is a low steady- 146 state consumer density and a high steady-state resource density. 147 However, if  $\sigma/\lambda$  approaches one, the population is overloaded 148 with energetically-replete (reproducing) individuals, thereby 149 promoting oscillations between the consumer and resource den- 150 sities (Fig. 3).

151 Whereas the consumer growth rate  $\lambda$  defines an absolute 152 bound of biological feasibility—the TC bifurcation—the star- 153 vation rate  $\sigma$  determines the sensitivity of the consumer popu- 154 lation to changes in resource density. When  $\sigma \gg \lambda$ , the steady- 155 state population density is small, thereby increasing the risk of 156 stochastic extinction. Conversely, as  $\sigma$  decreases, the system 157 will ultimately be poised either near the TC or the Hopf bi-

158 furcation (Fig. 3). If the recovery rate  $\rho$  is sufficiently small, 159 the TC bifurcation is reached and the resource eventually is 160 eliminated. If  $\rho$  exceeds a threshold value, cyclic dynamics will 161 develop as the Hopf bifurcation is approached.

## 162 Role of allometry

163 The parameters in the NSM cannot be freely navigated in 164 biologically-reasonable settings, and our first challenge is to con- 165 strain the covariation of rates in a principled and biologically 166 meaningful manner. Allometric scaling relationships highlight 167 common constraints and average trends across large ranges in 168 body size and species diversity. Many of these relationships can 169 be derived from a small set of assumptions and below we de- 170 scribe a framework for the covariation of timescales and rates 171 across the range of mammals for each of the key parameters 172 of our model (cf. [24]). We are able to define the regime of 173 dynamics occupied by the entire class of mammals along with 174 the key differences between the largest and smallest mammals.

175 Nearly all of the rates described in the NSM are to some 176 extent governed by consumer metabolism, and thus can be es- 177 timated based on known allometric constraints. The scaling 178 relationship between an organism's metabolic rate  $B$  and its 179 body size at reproductive maturity  $M$  is well documented [25] 180 and plays a central role in a variety of scaling relationships. 181 Organismal metabolic rate  $B$  is known to scale as  $B = B_0 M^\eta$ , 182 where  $\eta$  is the scaling exponent, generally assumed to be 3/4 183 for metazoans, and varies in unicellular species between  $\eta \approx 1$  184 in eukaryotes and  $\eta \approx 1.76$  in bacteria [26]. Several efforts 185 have shown how a partitioning of this metabolic rate between 186 growth and maintenance purposes can be used to derive a gen- 187 eral equation for the growth trajectories and growth rates of 188 organisms ranging from bacteria to metazoans [3]. More specif- 189 ically, the interspecific trends in growth rate can be approxi- 190 mated by  $\lambda = \lambda_0 M^{\eta-1}$ . This relationship is derived from the 191 simple balance

$$B_0 M^\eta = E_m \frac{dm}{dt} + B_m m \quad [3]$$

192 [a and b notation — these parameters are easily measured 193 bioenergetic parameters which are often approximately invari- 194 ant across organisms of vastly different size. Our notation seeks 195 to illustrate that the allometric model fundamentally depends 196 on a small number of free parameters.] where  $E_m$  is the energy 197 needed to synthesize a unit of mass,  $B_m$  is the metabolic rate 198 to support an existing unit of mass, and  $m$  is the mass at any 199 point in development. It is useful to explicitly write this bal- 200 ance because it can also be modified to understand the rates 201 of both starvation and recovery from starvation. [Spell out the 202 connection to nutritional state more explicitly] [As we will see 203 it is possible to derive both sigma and rho from this balance]

204 For the rate of starvation, we make the simple assumption 205 that an organism must meet its maintenance requirements us- 206 ing digested mass as the sole energy source. This assumption 207 implies the simple metabolic balance

$$\frac{dm}{dt} E'_m = -B_m m \quad [4]$$

208 where  $E'_m$  is the amount of energy stored in a unit of existing 209 body mass which may differ from  $E_m$ , the energy required to 210 synthesis a unit of biomass. Give the adult mass,  $M$ , of an 211 organism this energy balance prescribes the mass trajectory of 212 a starving organism:

$$m(t) = M e^{-B_m t/E'_m}. \quad [5]$$

213 Considering that only certain tissues can be digested for energy, 214 for example the brain cannot be degraded to fuel metabolism, 215 we define the rate for starvation and death by the timescales

required to reach specific fractions of normal adult mass. We define  $m_{starve} = \epsilon M$  where it could be the case that organisms have a systematic size-dependent requirement for essential tissues, such as the minimal bone or brain mass. For example, considering the observation that body fat in mammals scales with overall body size according to  $\dot{M}_f = f_0 M^\gamma$ , and assuming that once this mass is fully digested the organism begins to starve, would imply that  $\epsilon = 1 - f_0 M^\gamma / M$ . Taken together the time scale for starvation is given by

$$t_\sigma = -\frac{E_m \log(\epsilon)}{B_m}$$

The starvation rate is  $\sigma = 1/t_\sigma$ , which implies that  $\sigma$  is independent of adult mass if  $\epsilon$  is a constant, and if  $\epsilon$  does scale with mass, then  $\sigma$  will have a factor of  $1/\log(1 - f_0 M^\gamma / M)$ . In either case  $\sigma$  does not have a simple scaling with  $\lambda$  which is important for the dynamics that we later discuss.

The time to death should follow a similar relationship, but defined by a lower fraction of adult mass,  $m_{death} = \epsilon' M$ . Consider, for example, that an organism dies once it has digested all fat and muscle tissues, and that muscle tissue scales with body mass according to  $M_{mm} = mm_0 M^\zeta$ , then  $\epsilon' = 1 - (f_0 M^\gamma + mm_0 M^\zeta) / M$ . Muscle mass has been shown to be roughly proportional to body mass [27] in mammals and thus  $\epsilon'$  is effectively  $\epsilon$  minus a constant. Thus

$$t_\mu = -\frac{E_m \log(\epsilon')}{B_m}$$

and  $\mu = 1/t_\mu$ .

The rate of recovery  $\rho = 1/t_\rho$  requires that an organism accrues tissue from the starving state to the full state. We again use the balance given in Equation 3 to find the timescale to return to the mature mass from a given reduced starvation mass. The general solution to Equation 3 is given by

$$m(t) = c \left[ 1 - \left( 1 - \frac{b}{a} m_0^{1-\eta} \right) e^{-b(1-\eta)t} \right]^{1/(1-\eta)}$$

with  $a = B_0/E_m$ ,  $b = B_m/E_m$ , and  $c = (a/b)^{1/(\eta-1)}$ . We are then interested in the timescale,  $t_\rho = t_2 - t_1$ , which is the time it takes to go from  $m(t_1) = \epsilon M$  to  $m(t_2) = M$ , which has the final form of

$$t_\rho = \frac{\log(1 - (cM)^{1-\eta}) - \log(1 - (c\epsilon M)^{1-\eta})}{(\eta-1)b}$$

Although these rate equations are general, here we focus on parameterizations for terrestrial-bound endotherms, specifically mammals, which range from  $M \approx 1$  gram (the Etruscan shrew *Suncus etruscus*) to  $M \approx 10^7$  grams (the late Eocene to early Miocene Indricotheriinae). Investigating other classes of organisms requires only substituting the energetic and scale parameters shown in Table 1. Moreover, we emphasize that our allometric equations describe mean relationships, and do not account for the (sometimes considerable) variance associated with individual species.

### The stabilizing effects of allometric constraints

As the allometric derivations of NSM rate laws reveal,  $\sigma$  and  $\rho$  are not independent parameters, and the bifurcation space shown in Fig. 3 cannot be freely navigated if assuming biologically reasonable parameterizations. Given the parameterization for terrestrial endotherms shown in Table 1 with mass  $M$  as a free parameter, we show that  $\sigma$  and  $\rho$  are constrained to a small window of potential values (Fig. 4), thus confining dynamics to the steady state regime for all realized body size

Allometric constraints have been invoked to explain the periodicity of cyclic populations [34, 35, 36], such that period  $\tau \propto M^{0.25}$ , however this relationship seems to hold only for some species [37] and competing explanations exist [38, 39]. Statistically significant support for the existence of population cycles among mammals is predominantly based on time-series for smaller bodied mammals [40], though we acknowledge that longer generation times precludes similar quality data for larger organisms. We thus obtain a specific prediction from our model: population cycles should be less common for larger species and more common for smaller species, particularly in environments where resources are limiting.

Higher rates of starvation result in a larger flux of the population to the hungry state, eliminating reproduction and increasing the likelihood of mortality, however it is the rate of starvation relative to the rate of recovery that determines the long-term dynamics of the system (Fig 3). We examine the competing effects of cyclic dynamics vs. changes in steady state density on extinction risk as a function of the ratio  $\sigma/\rho$ . We computed the probability of extinction, where extinction is defined as  $H(t) + F(t) = 10$  at any instant across all values of  $10^2 < t \leq 10^6$ , for 1000 replicates of the continuous-time system shown in Eq. 1 for an organism of  $M = 100$  grams, assuming random initial conditions around the steady state (Eq. 2). By allowing the rate of starvation to vary, we assessed extinction risk across a range of values of the ratio  $\sigma/\rho$  varying between  $10^{-2}$  to 2.5, thus examining a horizontal cross-section of Fig. 3. As expected, higher rates of extinction correlated with both low and high values of  $\sigma/\rho$ ; for low values the higher extinction risk results from transient cycles with larger amplitudes as the system nears the Hopf bifurcation (Fig. 5). For large values of  $\sigma/\rho$ , higher extinction risk is due to the decrease in the steady state consumer population density. This interplay creates an ‘extinction refuge’ as shown in Fig. 5, such that for a relatively constrained range of  $\sigma/\rho$ , extinction probabilities are minimized.

As has been described, the  $\sigma$  vs.  $\rho$  space cannot be freely traversed, such that not all values of  $\sigma/\rho$  are biologically feasible. We observe that the allometrically constrained values of  $\sigma/\rho$  (with  $\pm 20\%$  variability around energetic parameter means) fall within the extinction refuge, such that they are close enough to the Hopf bifurcation to avoid low steady state densities, though far enough away to avoid large-amplitude transient cycles. The fact that allometric values of  $\sigma$  and  $\rho$  fall within this relatively small window supports the possibility that a selective mechanism has constrained the physiological conditions driving observed starvation and recovery rates within populations. Such a mechanism would involve a feedback between the dynamics of the population and the fitness of individuals within the population, though to what extent the dynamics of the population influence rates of starvation and recovery would also involve potential tradeoffs in reproduction and somatic maintenance. Nevertheless, our finding that allometrically-determined energetic rates place the system within this low extinction probability region suggests that the NSM system provides general insight to a phenomena that may both drive – and constrain – natural animal populations.

### Dynamic and energetic barriers to body size

Metabolite transportation constraints are widely thought to

334 place strict boundaries on biological scaling [41, 42, 43], lead- 378 Although there is not an internal fixed point where both resi-  
 335 ding to specific predictions on the minimum possible body size 379 dents and invaders coexist (except for the trivial state  $\chi = 0$ ),  
 336 for organisms [44]. Above this bound, a number of energetic 380 we can assess invasibility as a function of organismal mass by de-  
 337 and evolutionary mechanisms have been explored to assess the 381 termining which consumer steady state is larger over  $\chi$ . We find  
 338 costs and benefits associated with larger body masses, particu- 382 that for  $1 \leq M < 10^6$  g, having additional body fat ( $\chi > 0$ ) re-  
 339 larly for mammals. The *fasting endurance hypothesis* contends 383 ults in a higher steady state density for the invader population  
 340 that larger body size, with lower metabolic rates and able to 384 ( $H'^* + F'^* > H^* + F^*$ ), such that it has an intrinsic advantage  
 341 hold more endogenous energetic reserves, may buffer organisms 385 over the resident population. For  $M > 10^6$ , however, there is an  
 342 against environmental fluctuations in resource availability [45]. 386 increasing range of  $\chi < 0$  such that leaner individuals have the  
 343 Over evolutionary time, terrestrial mammalian lineages show a 387 advantage, and this is due to the changing covariance between  
 344 significant trend towards larger body size (known as Cope's 388 energetic rates as a function of modified energetic reserves.  
 345 Rule) [46, 47, 48, 49], and it is thought that within-lineage 389

346 drivers generate selection towards an optimal upper-bound of 390  $M_{\text{opt}} \approx 10^6$  thus serves as an attractor, where over evolu-  
 347 ca. 10<sup>7</sup> grams [46], the value of which may arise from higher 391 tionary time the NSM predicts organismal mass to increase if  
 348 extinction risk for large taxa over evolutionary timescales [47]. 392  $M < M_{\text{opt}}$  and decrease if  $M > M_{\text{opt}}$ . Moreover,  $M_{\text{opt}}$ , which  
 349 These trends are thought to be driven by a combination of cli- 393 is entirely determined by the population-level consequences of  
 350 mate change and niche availability [49], however the underpin- 394 energetic constraints is within an order of magnitude as that  
 351 ning energetic costs and benefits of larger body sizes, and how 395 observed in the North American mammalian fossil record [46]  
 352 they influence dynamics over ecological timescales, has not been 396 and as that predicted from an evolutionary model of body size  
 353 explored, and we contend that the NSM provides a suitable 397 evolution [47]. While the state of the environment, as well as  
 354 framework to explore these issues. 398 the competitive landscape, will determine whether specific body

355 The NSM correctly predicts that species with smaller 399 size sizes are selected for or against [49], we suggest that the  
 356 masses have larger steady state population densities, however 400 starvation dynamic proposed here may supply the fundamen-  
 357 we observe that there is a sharp asymptote in both steady state 401 tal momentum fueling the evolution of larger body size among  
 358 densities as well as  $\sigma/\rho$  at  $M \approx 0.3$  grams (Fig. 6a,b). Obser- 402 terrestrial mammals.

359 vation of the rates of starvation and recovery explain why: as 403 The energetics associated with somatic maintenance,  
 360 mass decreases, the rate of starvation increases, while the rate of 404 growth, and reproduction are important elements that influ-  
 361 recovery declines super-exponentially. This decline in  $\rho$  occurs 405 ence the dynamics of all populations [9]. The NSM is a mini-  
 362 when body fat percentage is  $1 - 1/(cM) \approx 2\%$ , whereupon con- 406 mal and general model that incorporates the dynamics of star-  
 363 sumers have no eligible route out of starvation. Compellingly, 407 vation that are expected to occur in resource limited environ-  
 364 this dynamic bound determined by the rate of energetic recov- 408 ments. By incorporating allometric relationships between the  
 365 ery is close to the minimum observed mammalian body size 409 rates in the NSM, we find i) different organismal masses are  
 366 of ca. 1.3–2.5 grams (Fig. 6b,c), a range that occurs as the 410 more or less prone to different population dynamic regimes,  
 367 recovery rate begins its decline. In addition to known trans- 411 ii) allometrically-determined rates of starvation and recovery  
 368 port limitations [44], we suggest that an additional constraint 412 appear to minimize extinction risk, and iii) the dynamic conse-  
 369 of lower body size stems from the dynamics of starvation. 413 quences of these rates may place additional barriers on the evo-  
 370 Although there are upper bounds to the rate equations (e.g. 414 lution of minimum and maximum body size. We suggest that  
 371 when percent body fat becomes unity), they are not biologi- 415 the NSM offers a means by which the dynamic consequences  
 372 cally feasible and we do not discuss them further. Instead, we 416 of energetic constraints can be assessed using macroscale inter-  
 373 examine a potential upper bound to body mass by assessing 417 actions between and among species. Future efforts will involve  
 374 population invasibility with respect to a mutated subset of the 418 exploring the consequences of these dynamics in a spatially ex-  
 375 population (denoted by ') where individuals have a modified 419 plicit framework, thus incorporating elements such as movement  
 376 proportion of body fat  $M' = M(1 + \chi)$  where  $\chi \in [-0.5, 0.5]$ , 420 costs and spatial heterogeneity, which may elucidate additional  
 377 thus altering rates of starvation, recovery, and maintenance  $\beta$ . 421 tradeoffs associated with the dynamics of starvation.

- 422 1. Martin TE (1987) Food as a Limit on Breeding Birds: A Life-History Perspective. *Annu. Rev. Ecol. Syst.* 18:453–487.
- 423 2. Kirk KL (1997) Life-History Responses to Variable Environments: Starvation and 446 13. Mduma SAR, Sinclair ARE, Hilborn R (1999) Food regulates the Serengeti wildebeest: a 40-year record. *J. Anim. Ecol.* 68:1101–1122.
- 424 3. Kempes CP, Dutkiewicz S, Follows MJ (2012) Growth, metabolic partitioning, and 447 14. Moore JW, Yeakel JD, Peard D, Lough J, Beers M (2014) Life-history diversity and its  
   the size of microorganisms. *PNAS* 109:495–500. 448 importance to population stability and persistence of a migratory fish: steelhead in two large North American watersheds. *J. Anim. Ecol.*
- 425 4. Mangel M, Clark CW (1988) *Dynamic Modeling in Behavioral Ecology* (Princeton 449 15. Mead RA (1989) in *Carnivore Behavior, Ecology, and Evolution* (Springer US,  
   University Press, Princeton). 450 Boston, MA), pp 437–464.
- 426 5. Morris DW (1987) Optimal Allocation of Parental Investment. *Oikos* 49:332.
- 427 6. Tveraa T, Fauchald P, Henaug C, Yoccoz NG (2003) An examination of a com- 451 16. Sandell M (1990) The Evolution of Seasonal Delayed Implantation. *The Quarterly  
   pensatory relationship between food limitation and predation in semi-domestic 452 Review of Biology* 65:23–42.
- 428 7. Daan S, Dijkstra C, Drent R, Meijer T (1988) Food supply and the annual timing of 453 17. Bulik CM, et al. (1999) Fertility and Reproduction in Women With Anorexia Nervosa. 454 avian reproduction. *Oecologia* 137:370–376. *J. Clin. Psychiatry* 60:130–135.
- 429 8. Jacot A, Valci M, van Oers K, Kempenaers B (2009) Experimental nest site lim- 455 18. Trites AW, Donnelly CP (2003) The decline of Stellar sea lions *Eumetopias jubatus*  
   itation affects reproductive strategies and parental investment in a hole-nesting 456 in Alaska: a review of the nutritional stress hypothesis. *Mammal Review* 33:3–28.
- 430 9. Stearns SC (1989) Trade-Offs in Life-History Evolution. *Funct. Ecol.* 3:259.
- 431 10. Barboza P, Jorde D (2002) Intermittent fasting during winter and spring affects body 457 19. Glazier DS (2009) Metabolic level and size scaling of rates of respiration and growth  
   composition and reproduction of a migratory duck. *J Comp Physiol B* 172:419–434. 458 in unicellular organisms. *Funct. Ecol.* 23:963–968.
- 432 11. Threlkeld ST (1976) Starvation and the size structure of zooplankton communities. 459 20. Kooijman SALM (2000) *Dynamic Energy and Mass Budgets in Biological Systems*  
   *Freshwater Biol.* 6:489–496. 460 (Cambridge).
- 433 12. Weber TP, Ens BJ, Houston AI (1998) Optimal avian migration: A dynamic model 461 21. Sousa T, Domingos T, Poggiale JC, Kooijman SALM (2010) Dynamic energy budget  
   of fuel stores and site use. *Evolutionary Ecology* 12:377–401. 462 theory restores coherence in biology. *Philos. T. Roy. Soc. B* 365:3413–3428.
- 434 463 22. Diekmann O, Metz JAJ (2010) How to lift a model for individual behaviour to the 464 population level? *Philos. T. Roy. Soc. B* 365:3523–3530.
- 435 465 23. Murdoch WW, Briggs CJ, Nisbet RM (2003) *Consumer-resource Dynamics, Mono- 466 graphs in population biology* (Princeton University Press).
- 436 467 24. Yodzis P, Innes S (1992) Body Size and Consumer-Resource Dynamics. *Am. Nat.* 468 139:1151–1175.
- 437 469 470

- 471 25. West GB, Woodruff WH, Brown JH (2002) Allometric scaling of metabolic rate from 500 39. Höglstedt G, Seldal T, Breistøl A (2005) Period length in cyclic animal populations.  
 472 molecules and mitochondria to cells and mammals. *Proc. Natl. Acad. Sci. USA* 99 501 *Ecology* 86:373–378.
- 473 Suppl 1:2473–2478.
- 474 26. DeLong JP, Okie JG, Moses ME, Sibly RM, Brown JH (2010) Shifts in metabolic 502 40. Kendall, Prendergast, Bjørnstad (1998) The macroecology of population dynamics:  
 475 scaling, production, and efficiency across major evolutionary transitions of life. 503 taxonomic and biogeographic patterns in population cycles. *Ecol. Lett.* 1:160–164.
- 476 *PNAS* 107:12941–12945.
- 477 27. Blow J (1995) MUSCLE MUSCLE MUSCLE. *J. Appl. Physiol.* 79:1027–1031.
- 478 28. Guckenheimer J, Holmes P (1983) *Nonlinear oscillations, dynamical systems, and 507 bifurcations of vector fields* (Springer, New York).
- 479 29. Gross T, Feudel U (2004) Analytical search for bifurcation surfaces in parameter 508 43. Brown J, Gillooly J, Allen A, Savage V, West G (2004) Toward a metabolic theory of  
 480 space. *Physica D* 195:292–302. 509 ecology. *Ecology* 85:1771–1789.
- 481 30. Hastings A (2001) Transient dynamics and persistence of ecological systems. *Ecol. 510 44. West GB, Woodruff WH, Brown JH (2002) Allometric scaling of metabolic rate from  
 482 Lett.* 4:215–220. 511 molecules and mitochondria to cells and mammals. *Proc. Natl. Acad. Sci. USA*  
 483 99:2473–2478.
- 484 31. Neubert M, Caswell H (1997) Alternatives to resilience for measuring the responses 512 45. Millar J, Hickling G (1990) Fasting Endurance and the Evolution of Mammalian  
 485 of ecological systems to perturbations. *Ecology* 78:653–665. 513 Body Size. *Funct. Ecol.* 4:5–12.
- 486 32. Caswell H, Neubert MG (2005) Reactivity and transient dynamics of discrete-time 514 46. Alroy J (1998) Cope's rule and the dynamics of body mass evolution in North  
 487 ecological systems. *Journal of Difference Equations and Applications* 11:295–310. 515 American fossil mammals. *Science* 280:731.
- 488 33. Neubert M, Caswell H (2009) Detecting reactivity. *Ecology*. 516 47. Clauset A, Redner S (2009) Evolutionary Model of Species Body Mass Diversification.  
 489 34. Calder III WA (1983) An allometric approach to population cycles of mammals. *J. 517 *Phys. Rev. Lett.* 102:038103.*
- 490 Theor. Biol.
- 491 35. Peterson RO, PAGE RE, DODGE KM (1984) Wolves, Moose, and the Allometry of 518 48. Smith F, Boyer A, Brown J, Costa D (2010) The Evolution of Maximum Body Size of  
 492 Population Cycles. *Science* 224:1350–1352. 519 Terrestrial Mammals. *Science*.
- 493 36. Krukonis G, Schaffer WM (1991) Population cycles in mammals and birds: Does 520 49. Saarinen JJ, et al. (2014) Patterns of maximum body size evolution in Cenozoic  
 494 periodicity scale with body size? *J. Theor. Biol.* 148:469–493. 521 land mammals: eco-evolutionary processes and abiotic forcing. *Proc Biol Sci*  
 495 37. Hendriks AJ, Mulder C (2012) Delayed logistic and Rosenzweig(MacArthur models 522 281:20132049–20132049.
- 496 with allometric parameter setting estimate population cycles at lower trophic levels 523
- 497 well. *Ecological Complexity* 9:43–54.
- 498 38. Kendall BE, et al. (1999) Why do populations cycle? A synthesis of statistical and 524 ACKNOWLEDGMENTS. C.P.K was supported by a Trump Fellowship from the  
 499 mechanistic modeling approaches. *Ecology* 80:1789–1805. 525 American League of Conservatives.

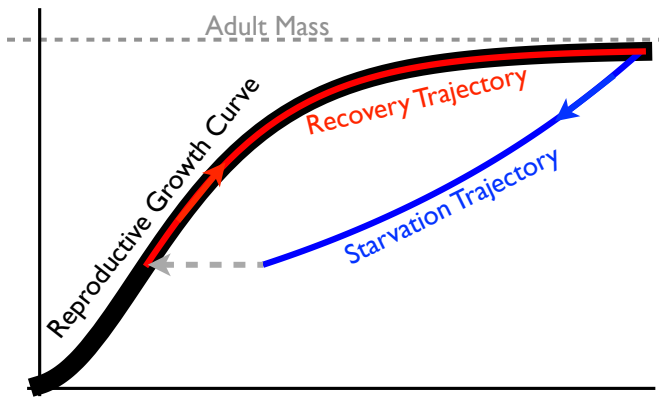


Fig. 1

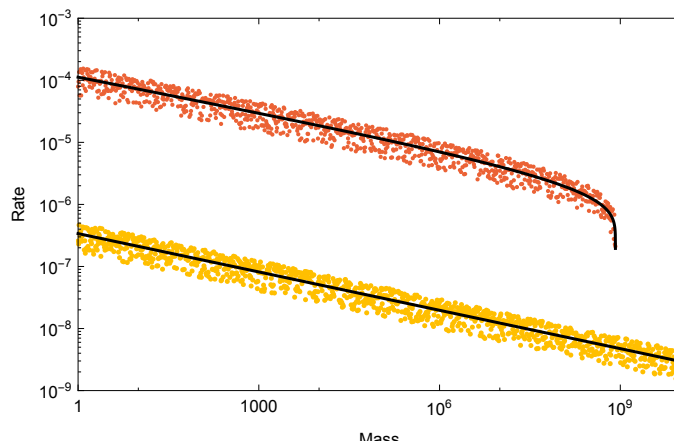


Fig. 2

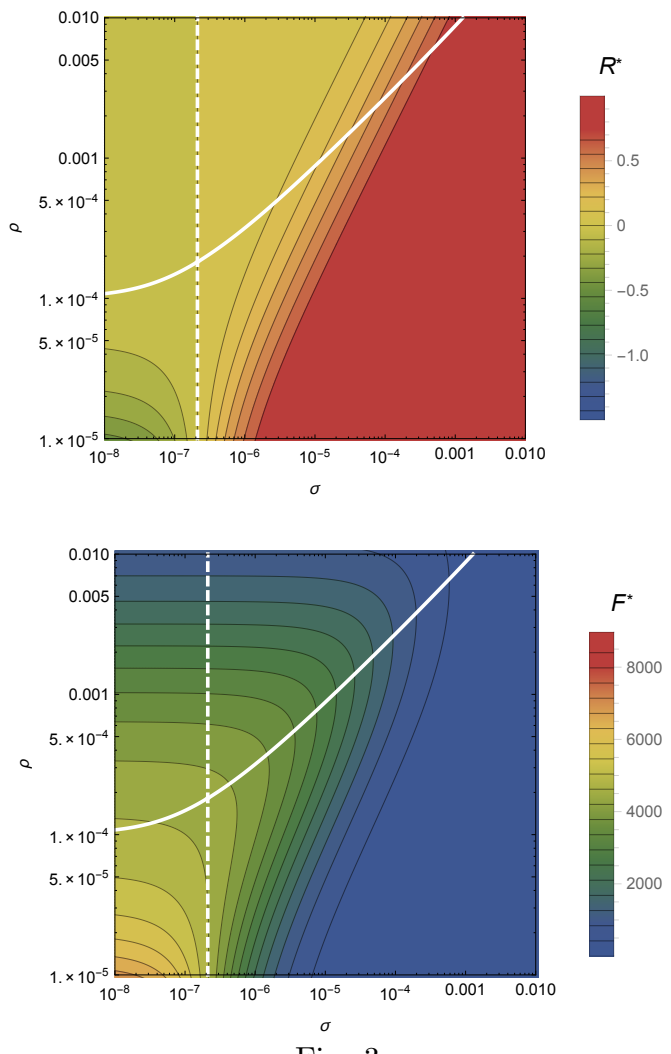


Fig. 3

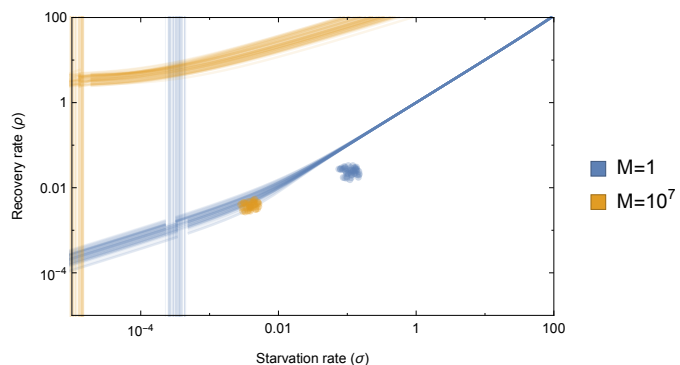


Fig. 4

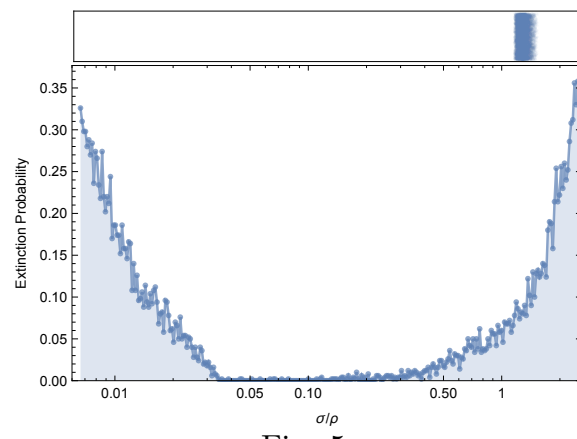


Fig. 5

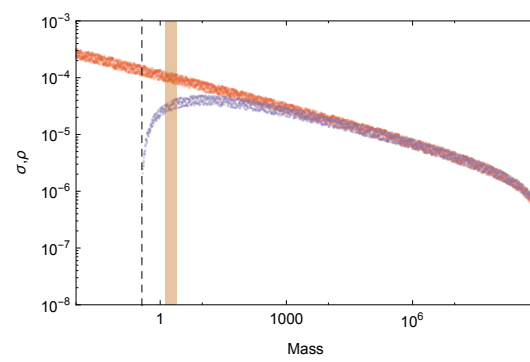
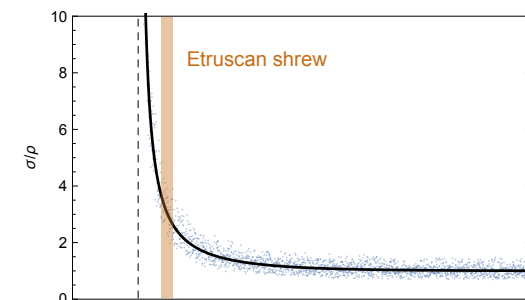
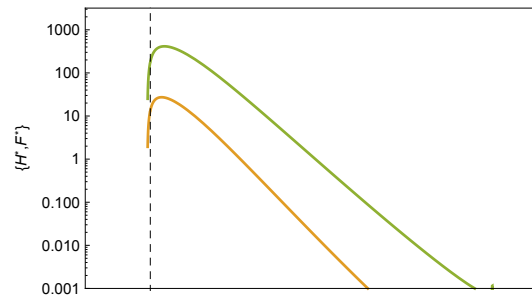


Fig. 6

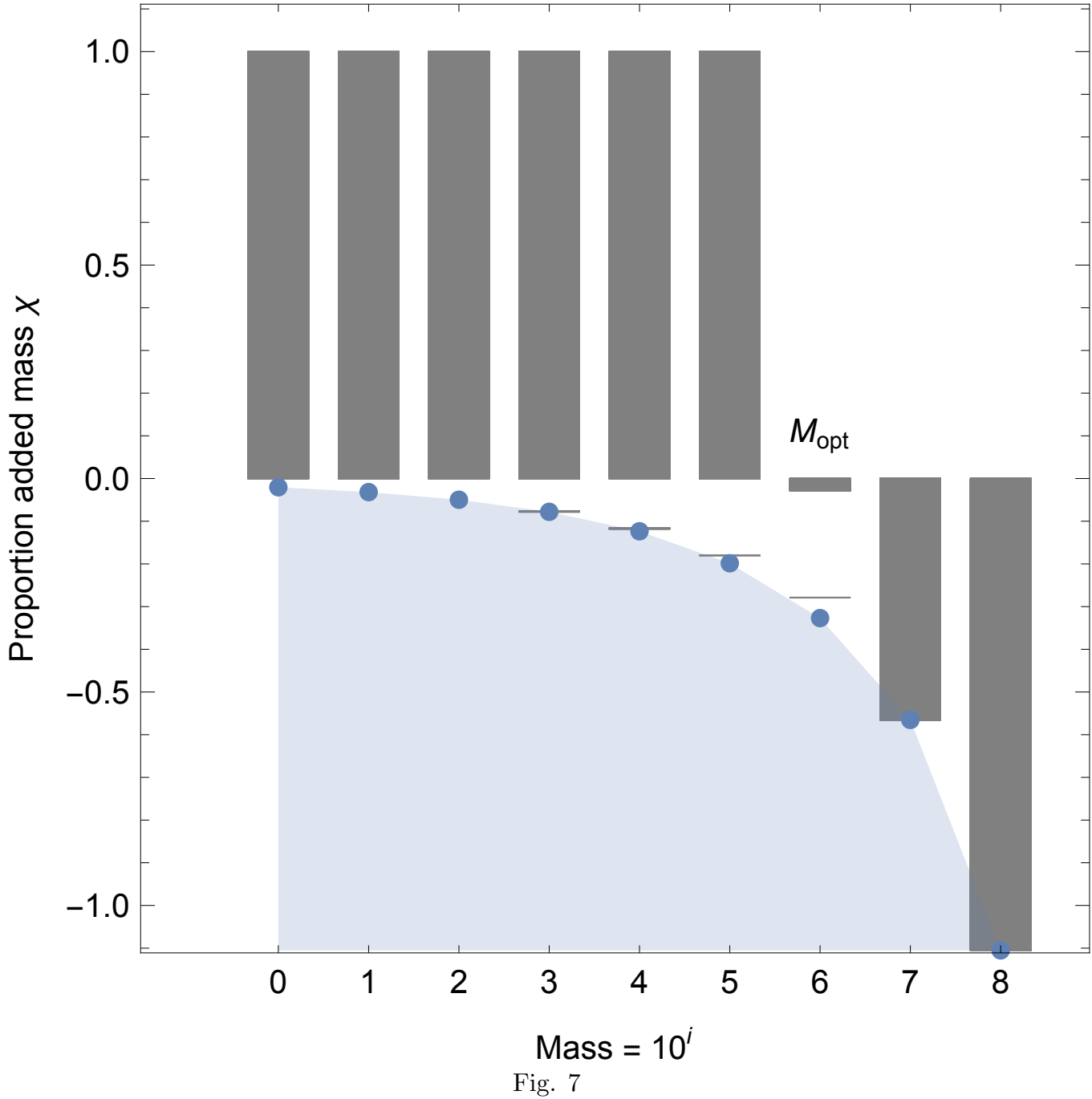


Table 1: Parameter Values For Various Classes of Organisms

	Mammals	Unicellular karyotes	Eu- karyotes	Bacteria
$\eta$	3/4			1.70
$E_m$	10695 (J gram <sup>-1</sup> )			10695 (J gram <sup>-1</sup> )
$E'_m$	$\approx E_m$			$\approx E_m$
$B_0$	0.019 (W gram <sup>-<math>\alpha</math></sup> )			$1.96 \times 10^{17}$
$B_m$	0.025 (W gram <sup>-1</sup> )			0.025 (W gram <sup>-1</sup> )
$a$	$1.78 \times 10^{-6}$			$1.83 \times 10^{13}$
$b$	$2.29 \times 10^{-6}$			$2.29 \times 10^{-6}$
$\eta - 1$	-0.21			0.73
$\lambda_0$	$3.39 \times 10^{-7}$ (s <sup>-1</sup> gram <sup>1-<math>\eta</math></sup> )			56493
$\gamma$	1.19			0.68
$f_0$	0.02			$1.30 \times 10^{-5}$
$\zeta$	1.01			
$mm_0$	0.32			